



NRC Publications Archive Archives des publications du CNRC

Expanding the repertoire of molecular linkages to silicon: Si–S, Si–Se, and Si–Te Bonds

Hu, Minjia; Liu, Fenglin; Buriak, Jillian M.

This publication could be one of several versions: author's original, accepted manuscript or the publisher's version. /
La version de cette publication peut être l'une des suivantes : la version prépublication de l'auteur, la version
acceptée du manuscrit ou la version de l'éditeur.

For the publisher's version, please access the DOI link below. / Pour consulter la version de l'éditeur, utilisez le lien
DOI ci-dessous.

Publisher's version / Version de l'éditeur:

<https://doi.org/10.1021/acsami.6b00784>

ACS Applied Materials & Interfaces, 8, 17, pp. 11091-11099, 2016-04-07

NRC Publications Record / Notice d'Archives des publications de CNRC:

<https://nrc-publications.canada.ca/eng/view/object/?id=c1c1a44d-27a8-422d-80b6-47aff6cbb712>

<https://publications-cnrc.canada.ca/fra/voir/objet/?id=c1c1a44d-27a8-422d-80b6-47aff6cbb712>

Access and use of this website and the material on it are subject to the Terms and Conditions set forth at

<https://nrc-publications.canada.ca/eng/copyright>

READ THESE TERMS AND CONDITIONS CAREFULLY BEFORE USING THIS WEBSITE.

L'accès à ce site Web et l'utilisation de son contenu sont assujettis aux conditions présentées dans le site

<https://publications-cnrc.canada.ca/fra/droits>

LISEZ CES CONDITIONS ATTENTIVEMENT AVANT D'UTILISER CE SITE WEB.

Questions? Contact the NRC Publications Archive team at

PublicationsArchive-ArchivesPublications@nrc-cnrc.gc.ca. If you wish to email the authors directly, please see the
first page of the publication for their contact information.

Vous avez des questions? Nous pouvons vous aider. Pour communiquer directement avec un auteur, consultez la
première page de la revue dans laquelle son article a été publié afin de trouver ses coordonnées. Si vous n'arrivez
pas à les repérer, communiquez avec nous à PublicationsArchive-ArchivesPublications@nrc-cnrc.gc.ca.



Expanding the Repertoire of Molecular Linkages to Silicon: Si–S, Si–Se, and Si–Te Bonds

Minjia Hu,^{†,‡} Fenglin Liu,^{†,‡} and Jillian M. Buriak^{*,†,‡}

[†]Department of Chemistry, University of Alberta, 11227 Saskatchewan Drive, Edmonton, Alberta T6G 2G2, Canada

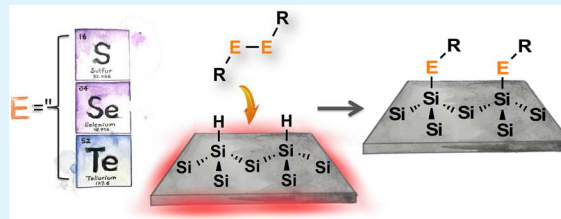
[‡]National Institute for Nanotechnology, National Research Council Canada, 11421 Saskatchewan Drive, Edmonton, Alberta T6G 2M9, Canada

S Supporting Information

ABSTRACT: Silicon is the foundation of the electronics industry and is now the basis for a myriad of new hybrid electronics applications, including sensing, silicon nanoparticle-based imaging and light emission, photonics, and applications in solar fuels, among others. From interfacing of biological materials to molecular electronics, the nature of the chemical bond plays important roles in electrical transport and can have profound effects on the electronics of the underlying silicon itself, affecting its work function, among other things. This work describes the chemistry to produce $\equiv\text{Si}-\text{E}$ bonds

(E = S, Se, and Te) through very fast microwave heating (10–15 s) and direct thermal heating (hot plate, 2 min) through the reaction of hydrogen-terminated silicon surfaces with dialkyl or diaryl dichalcogenides. The chemistry produces surface-bound $\equiv\text{Si}-\text{SR}$, $\equiv\text{Si}-\text{SeR}$, and $\equiv\text{Si}-\text{TeR}$ groups. Although the interfacing of molecules through $\equiv\text{Si}-\text{SR}$ and $\equiv\text{Si}-\text{SeR}$ bonds is known, to the best of our knowledge, the heavier chalcogenide variant, $\equiv\text{Si}-\text{TeR}$, has not been described previously. The identity of the surface groups was determined by Fourier transform infrared (FTIR) spectroscopy, X-ray photoelectron spectroscopy (XPS), and depth profiling with time-of-flight-secondary ionization mass spectrometry (ToF-SIMS). Possible mechanisms are outlined, and the most likely, based upon parallels with well-established molecular literature, involve surface silyl radicals or dangling bonds that react with either the alkyl or aryl dichalcogenide directly, REER, or its homolysis product, the alkyl or aryl chalcogenyl radical, RE· (where E = S, Se, and Te).

KEYWORDS: silicon, surface, chalcogenide, sulfur, selenium, tellurium, radical



INTRODUCTION

Silicon as a material dominates the microelectronic industry because of its ideal band gap, oxide surface chemistry, and etching properties that enable the manufacture of incredibly powerful integrated circuitry.^{1,2} Functionalization of silicon surfaces through the grafting of organic and biologically sourced molecules is of significance for practical applications that take advantage of the electronic platform of a silicon chip, as well as the versatility of organic and bioorganic chemistry.^{3,4} Examples of silicon-based devices include light absorbers based on silicon for generation of solar fuels,⁵ silicon nanoparticle-based imaging and drug delivery,^{6,7} applications in molecular electronics,^{8–10} chemical sensing and biosensing,^{11,12} photonics,^{13,14} and many other applications.^{15,16}

The nature of the connection to silicon for electronic applications is critical as the chemical identity of this linkage can have profound effects on the electronics of the underlying semiconductor.^{17,18} For instance, the junction resistance of silicon-based solar generators can be reduced by surface functionalization, thus optimizing the electrical transport throughout the system.⁵ The thickness of a self-assembled monolayer (SAM) or the length of molecular wires on a functionalized surface will also have a significant impact on electron-transport mechanisms.¹⁹ For quantum dots composed

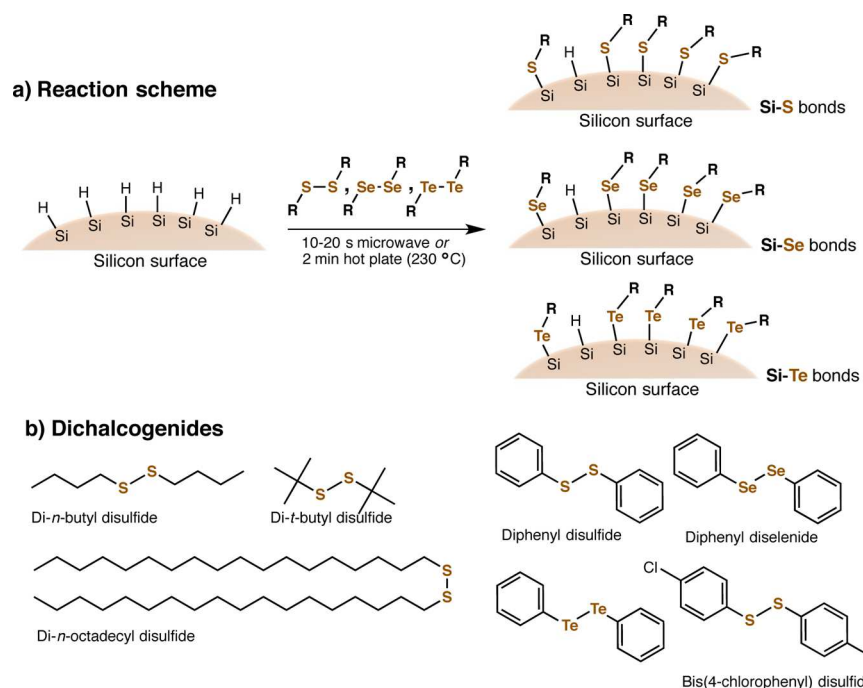
of crystalline silicon, the chemical nature of the silicon interface greatly affects the underlying electronics, thus modulating the wavelength of emission of photoluminescence.^{13,20} Underlying the observed electronic effects, recent experimental and theoretical results have provided insights into the fundamentals and have shown that the work function of silicon surfaces can be tuned through the choice of head groups through which a self-assembled monolayer (SAM) can be bonded.^{21,22} Fagas and co-workers predict that tuning of the work function by up to 1.73 eV is possible through tailoring of the chemical nature of the SAM as a result of modulation of surface dipoles.²³ Bonding of SAMs through Si–O, Si–S, Si–Se, Si–Te, and Si–N bonds as well as SiX (X = halide) coverage were examined; for heavier atoms (Te versus Se versus S versus O), additional electronic states are available, which can affect electron transfer to and from molecules attached to a silicon surface.^{21,24}

In contrast to the vast literature of SAMs bonded to silicon through $\equiv\text{Si}-\text{C}$ ^{25,26} and $\equiv\text{Si}-\text{O}$ linkages,^{27,28} the development of silicon–chalcogenide bond-forming reaction schemes on silicon surfaces has only just begun, in spite of the strong

Received: January 20, 2016

Accepted: April 7, 2016

Published: April 7, 2016

Scheme 1. Reaction Approach To Functionalize Silicon^a

^a(a) Overall reaction scheme outlining the approach to Si–S, Si–Se, and Si–Te bond formation on silicon surfaces. (b) Seven dichalcogenide molecules that were screened for reactivity under microwave irradiation or direct thermal heating (hot plate) on hydrogen-terminated porous silicon.

impetus to study, understand, and apply them. The field of Si–S- and Si–Se-based SAMs on surfaces via solution (non-vacuum) chemistry can be summarized in one paragraph. The first literature report of $\equiv\text{Si}-\text{SR}$ bond formation on hydrogen-terminated flat was driven by UV irradiation in the presence of alkanethiols.^{29–31} 1-Dodecanethiol forms monolayers on Si(111)–H with 2–4 h of illumination with UV light^{29,31} or 90 min of white light.³⁰ 1-Octadecanethiol was shown to react with Si(111)–H at 150 °C, overnight when used as a solution³² or within 1–2 h when applied neat.³³ Acetylchalcogenidoarene-derivatized (Ar–EAc, E = O, S, and Se) porphyrins can be covalently attached to silicon surfaces via $\equiv\text{Si}-\text{S}$ and $\equiv\text{Si}-\text{Se}$ bonds through a 2 min high-temperature reaction at 400 °C.^{34,35} Recently, Korgel and co-workers showed that silicon nanoparticles could be functionalized with a monolayer of $\equiv\text{Si}-\text{S}-n$ -dodecyl through a 12 h thermal reaction at 190 °C.³⁶ Our group showed how porous silicon could be functionalized through a room-temperature radical-initiated process using dialkyl and diaryl disulfides and diselenides, but the chemistry did not proceed with sterically hindered disulfides (i.e., with *t*-butyl substituents) or ditellurides (the latter because of very low solubility).³⁷ Finally, to the best of our knowledge, there are no reports of SAMs attached to silicon through $\equiv\text{Si}-\text{Te}$ bonds. To summarize, the chemistry of silicon-chalcogenide-based interfacing of molecules on silicon surfaces is still in very early stages when compared to the richness of the literature pertaining to silicon–carbon and silicon–oxygen bond formation.

Here, we describe 15-s to 2-min functionalization chemistry of readily accessible and commercially available dichalcogenide molecules, those containing S–S, Se–Se, and Te–Te bonds, with hydrogen-terminated silicon (Scheme 1). These dialkyl and diaryl dichalcogenide molecules are practical to work with and are far less odorous than the corresponding chalcogenols (thiols and selenols). In the case of the tellurium compounds,

unhindered tellurols are unstable,^{38,39} whereas the ditellurides are stable and easy to work with.⁴⁰ Thus, the direct reaction with the ditellurides may be one of the only viable routes to SAMs based upon Si–Te bonds. The reactions are driven by either microwave irradiation in 15 s or less or on a hot plate in 2 min or less. Comparison with the molecular literature of silanes and chalcogenides provides insights into the mechanism.

■ MATERIALS AND METHODS

General. Silicon wafers (100, prime-grade, n-type, P-doped, 1–3 $\Omega\cdot\text{cm}$, $450 \pm 25 \mu\text{m}$) were obtained from Virginia Semiconductor, Inc. Di-*n*-butyl disulfide (97%), di-*t*-butyl disulfide (97%), diphenyl disulfide (99%), diphenyl diselenide (98%), diphenyl ditelluride (98%), bis(4-chlorophenyl) disulfide (97%), 1-octadecanethiol (98%), *t*-butylthiol (2-methyl-2-propanethiol, 99%), and aluminum oxide (activated, neutral, Brockmann Neutral I, standard grade, ~ 150 mesh, 58 Å) were purchased from Sigma-Aldrich. Alumina was dried in a 100 °C oven for more than 24 h before being transferred to glovebox while still hot. Di-*n*-octadecyl disulfide (98%) was purchased from Alfa Aesar. All the reagents were stored at –20 °C inside an argon-filled glovebox. Molecular sieves (type 4A, 1/16 in. pellets, for selective adsorption) were purchased from Caledon Laboratories, Ltd. Ethanol (absolute) and acetone (reagent) were purchased from Fisher. HF (aqueous, 49%, semiconductor grade) was purchased from J. T. Baker. Degassed and dry dichloromethane was obtained from a solvent purification system (Innovative Technologies, Inc.), taken into glovebox in a standard dry Schlenk flask, and dried over molecular sieve for 24 h in glovebox prior to use. All liquid chemicals were passed through a fresh column of alumina prior to use in the glovebox.

Porous Silicon Preparation. Porous silicon was prepared according the method previously described in the literature.^{41,42} Silicon wafers were cut into 1.4 cm² (1.2 cm \times 1.2 cm) pieces,

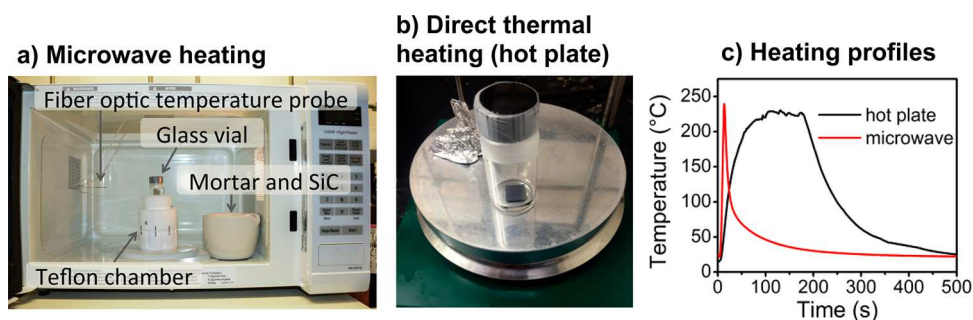


Figure 1. (a) Photograph of the microwave heating apparatus, comprised of a microwave for domestic use, a fiber optic temperature probe, and the sample vial residing within the Teflon chamber. (b) Photograph of direct thermal heating apparatus (hot plate). (c) Temperature profiles for the heating rates of $1.2 \times 1.2 \text{ cm}^2$ porous silicon samples that were heated in absence of reagents under microwave and direct heating. Temperature profiles were determined on dummy porous silicon samples in the absence of reagents because the vials are sealed to prevent contamination, oxidation, and damage to the polyimide probe.

cleaned by sonication (10 min in 1:1 acetone/ethanol), rinsed with ethanol, and dried with an argon stream. The unpolished side of the silicon wafer was in contact with an aluminum foil tongue electrode to act as the anode and a Pt wire loop electrode was used as the cathode. Using a 24.5% HF/25.5% $\text{H}_2\text{O}/50\%$ EtOH solution as electrolyte/etchant, the silicon was anodized at 7.6 mA cm^{-2} for 90 s and then 76 mA cm^{-2} for 120 s with full white-light illumination ($\sim 40 \text{ mW cm}^{-2}$) using an ELH bulb. The freshly etched silicon was rinsed with excess ethanol, immersed in pentane, then dried with an argon stream, and stored in an argon-filled airtight glass vial in the dark.

Determination of Heating Rate and Profile. The heating rate and heating profiles of the porous silicon samples were determined before the actual chemical reaction on dummy porous silicon samples, without the dichalcogenide or thiol reagents, because of the potential of reactivity of the polyimide fluorescence optical fiber temperature sensor with these reagents (vide infra). Thus, a porous silicon sample was prepared in identical fashion and was heated under the same conditions to determine heating rate and heating profile. The fiber optic probe cannot exceed $250 \text{ }^\circ\text{C}$ without succumbing to permanent damage.

Reactions under microwave irradiation were performed in a modified domestic Panasonic microwave oven (model number NNST651W, purchased from Walmart), as described previously.⁴³ A mortar containing 100 g of SiC powder (200–450 mesh, purchased from Sigma-Aldrich) was placed in the right side of microwave oven to absorb excess microwave radiation and prevent damage to the microwave. A fluorescence-based fiber optic temperature probe (model number PRB-G40–2.0M-ST-C with polyimide tip and calibration to $250 \text{ }^\circ\text{C}$ and accuracy of $\pm 0.5 \text{ }^\circ\text{C}$ obtained from OSENSA Inc.) was inserted through small holes drilled in the side of the microwave oven and Teflon chamber (Figure S23a and ref 43). A freshly prepared porous silicon piece was placed in a Teflon chamber, and the fiber optic probe was placed in direct physical contact with the silicon for in situ monitoring (Figure 1a). When the temperature of the wafer reached $240 \text{ }^\circ\text{C}$, the microwave oven was shut off manually. The temperature profile is plotted in Figure 1c. After the microwave oven was turned on, a 4 s lag was required to activate the cavity magnetron, so the temperature of the silicon wafers did not change in the first 4 s. After 4 s, the silicon wafer would undergo an increase in temperature to reach $240 \text{ }^\circ\text{C}$ in 12 s, and then the microwave oven was shut off manually, followed by a cooling down of the wafer; after reaching $240 \text{ }^\circ\text{C}$ in 12 s, the sample cooled to $50 \text{ }^\circ\text{C}$

in 88 s and, if followed for longer periods of time, reached $30 \text{ }^\circ\text{C}$ in 198 s. The temperature was monitored and recorded until the wafer had cooled to around $25 \text{ }^\circ\text{C}$. It is assumed that samples irradiated for longer than 12 s will increase further in temperature, above $240 \text{ }^\circ\text{C}$.

Determination of the heating profile of porous silicon on a hot plate was carried out by placing a fiber optic probe in direct contact with a porous silicon wafer inside of the same type of glass vial used for the experiments with chalcogenide. A small hole was, however, drilled into the vial to enable the fiber optic probe to be threaded through the hole to make direct contact with the dummy piece of porous silicon (Figure S23b). The hot plate temperature was set to $250 \text{ }^\circ\text{C}$. After 2 min, the wafer and the probe were removed from the hot plate. The temperature was monitored and recorded until the wafer had cooled to around $25 \text{ }^\circ\text{C}$.

Reactions with the Dichalcogenides and Thiols. Before carrying out each reaction, the liquid molecules to be used, including the di-*n*-butyl disulfide, di-*t*-butyl disulfide, and *t*-butylthiol were passed through a fresh column of alumina before use. Solids (generally the diaryl dichalcogenides) were used with no further purification. Twenty drops of liquid reagent or for solids, about 0.05 g, were placed on a porous silicon substrate, inside a 20 mL glass vial. The melting points of all the solids used here were lower than the maximum temperature reached, and thus they would liquefy in situ. For instance, the melting points of PhEePh are $61 \text{ }^\circ\text{C}$ ($\text{E} = \text{S}$), $61 \text{ }^\circ\text{C}$ ($\text{E} = \text{Se}$), and $66 \text{ }^\circ\text{C}$ ($\text{E} = \text{Te}$). The face of the silicon with the etched porous silicon was placed upside down to enforce spreading of the reagent, thus forming a sandwich of glass–reagent–porous silicon. The glass vials were then sealed with multilayers of parafilm entwined round the cap to seal (Figure 1a,b).

For the microwave reaction, the sealed glass vial containing reagent and porous silicon substrate was removed from glovebox and put in the center of a Teflon chamber, which was marked and fixed in the center of the microwave oven (Figure 1a), followed by microwave irradiation. When the microwave oven was shut off, the glass vial was transferred to the glovebox for rinsing. For the hot plate reactions, the sealed glass vial containing the reagent and the porous silicon substrate was put on a $250 \text{ }^\circ\text{C}$ hot plate for the desired reaction time (Figure 1b). After reactions (microwave or hot plate), the porous silicon samples were soaked in dry dichloromethane for 5 min and rinsed three times with a forceful stream of dry dichloromethane from a pipet to remove

excess unreacted reagents. The samples were removed from the glovebox (in the sealed glass vial), dried with argon gas, and then analyzed.

Analytical Techniques. Scanning electron microscopy (SEM) images were obtained with a Hitachi S-4800 FE-SEM with an accelerating voltage of 15 kV. FTIR spectra were collected with a Nicolet Nexus 760 spectrometer with a liquid-nitrogen-cooled MCT detector and a nitrogen-purged sample chamber (32 scans, 4 cm^{-1} resolution). X-ray photoelectron spectroscopy (XPS) was taken on a Kratos Axis 165 X-ray photoelectron spectrometer in the Alberta Centre for Surface Engineering and Science (ACES), now part of the University of Alberta NanoFAB. Time-of-flight secondary ion mass spectroscopy (TOF-SIMS) depth analysis was obtained on a ToF-SIMS IV-100 (ION-TOF GmbH) at ACES. The pSi samples were sputtered with a 1 keV Cs^+ ion source, leading to a crater size of 150 $\mu\text{m} \times 150 \mu\text{m}$, with analysis by Ga^+ at 25 keV, 35 $\mu\text{m} \times 35 \mu\text{m}$.

RESULTS AND DISCUSSION

Hydrogen-Terminated Surfaces. Porous silicon was applied as the test bed for surface chemistry development because it enables exquisite analysis by FTIR, XPS, and depth profiling using techniques such as ToF-SIMS, among others.^{44,45} The surface of hydride-terminated porous silicon is closely related to those of other hydride-terminated nanocrystalline surfaces (silicon nanocrystals, for example), as well as hydride-terminated Si(100), because they are capped by Si-H, Si-H₂, and Si-H₃ groups; their FTIR spectra, as a result, are very similar.^{46–48} Porous silicon was electrochemically etched from single-crystal Si(100) wafers with ethanolic HF (aqueous) to provide high-surface-area, hydride-terminated silicon samples whose surface is essentially oxide-free.^{41,42} The chemistry of porous silicon is closely related to the reactivity of other hydride-terminated flat and nanocrystalline surfaces; thus, observed reactions are typically generalizable to other morphologies.^{44,49} Because hydrogen-terminated silicon surfaces are metastable in laboratory ambient (air, room temperature) and can resist oxidation on a time scale of minutes, they are an ideal interface for more sophisticated functionalization of silicon. Si-H-terminated surfaces are, however, still sensitive with respect to low concentrations of dissolved oxygen, particularly under conditions required to promote functionalization (heat, illumination, radical initiators, for instance), and so even very low oxygen levels (ppm) can effectively compete with the desired chemistry, leading to mixed oxide surfaces.⁵⁰ To favor efficient and clean reactions and to compete with oxidation, neat reagents and very short reaction times were preferred.

Rapid Silicon–Chalcogen Bond Formation. As shown in Scheme 1, the reaction approach to functionalize the silicon involves rapid thermal heating of a dialkyl or diaryl dichalcogenide, a molecule containing a S–S, Se–Se, or Te–Te bond, with hydride-terminated porous silicon. A small quantity of the neat dichalcogenide molecule was placed on the porous silicon in a glass vial under inert atmosphere (inside an argon-filled glovebox, and sealed) and then placed in a standard domestic microwave for 10–15 s or on a hot plate set to 250 °C for 2 min, as outlined in Figure 1. The use of microwave irradiation to promote heating on silicon is well-established; it is known that lightly doped silicon wafers heat up rapidly upon microwave irradiation, that the rate of heating is dependent upon doping levels, and that in the extreme case silicon can

reach melting temperatures.⁴³ Boukherroub and co-workers used microwave irradiation to reduce the time required for alkene hydrosilylation on lightly doped porous silicon from hours to about 10 min.⁵¹ In this work, 1.2 \times 1.2 cm^2 samples of n-type, P-doped, 1–3 $\Omega\text{-cm}$ Si(100) reach 240 °C in approximately 10–12 s with microwave irradiation, as monitored with a fiber optic temperature probe in direct contact with the silicon. In the second approach to heating, the same sample size of porous silicon in a glass vial is placed onto a hot plate set to 250 °C; monitoring of the temperature with the fiber optic probe shows that it takes approximately 100 s to reach 230 °C (Figure 1c).

Scheme 1 shows the seven dialkyl and diaryl dichalcogenide molecules examined in this work. Analysis of the microwave and hot plate reactions was first carried out by transmission mode FTIR (Figure 2). In all cases, the reactions were carried out for different lengths of time, and the best spectra, in terms of low oxidation and high incorporation levels, are shown in the

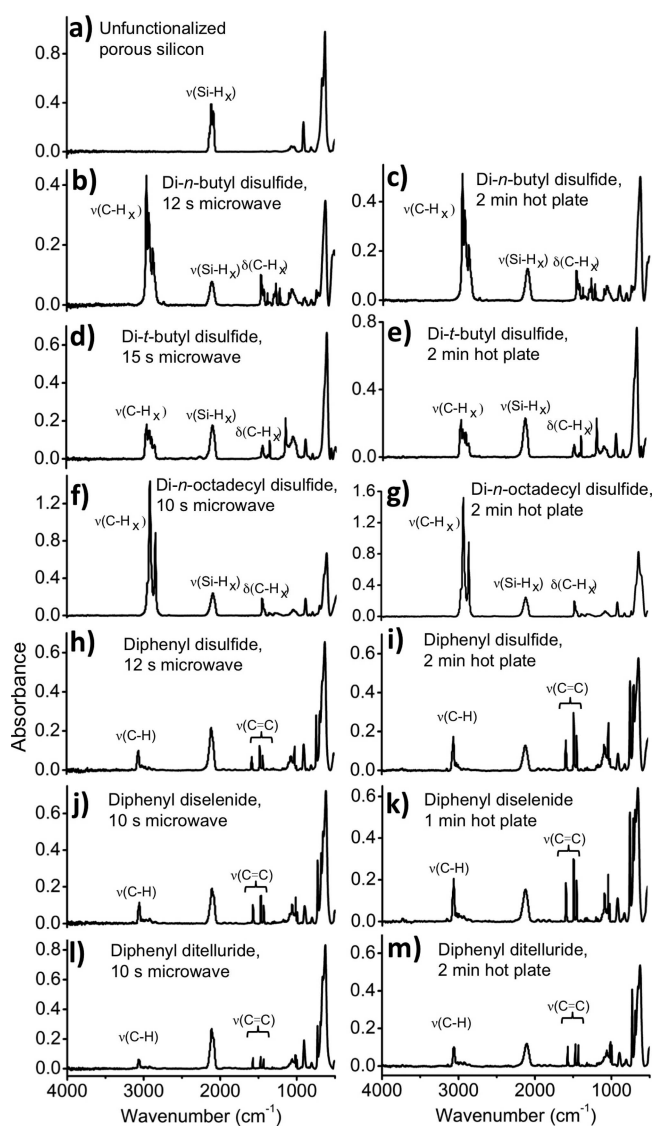


Figure 2. FTIR spectra (transmission mode) of (a) freshly etched unfunctionalized porous silicon and (b–m) porous silicon samples reacted with the chalcogenide reagents and time indicated under microwave irradiation (left) and hot plate heating (right). Hot plate temperature was set to 250 °C; sample temperature reaches 230 °C.

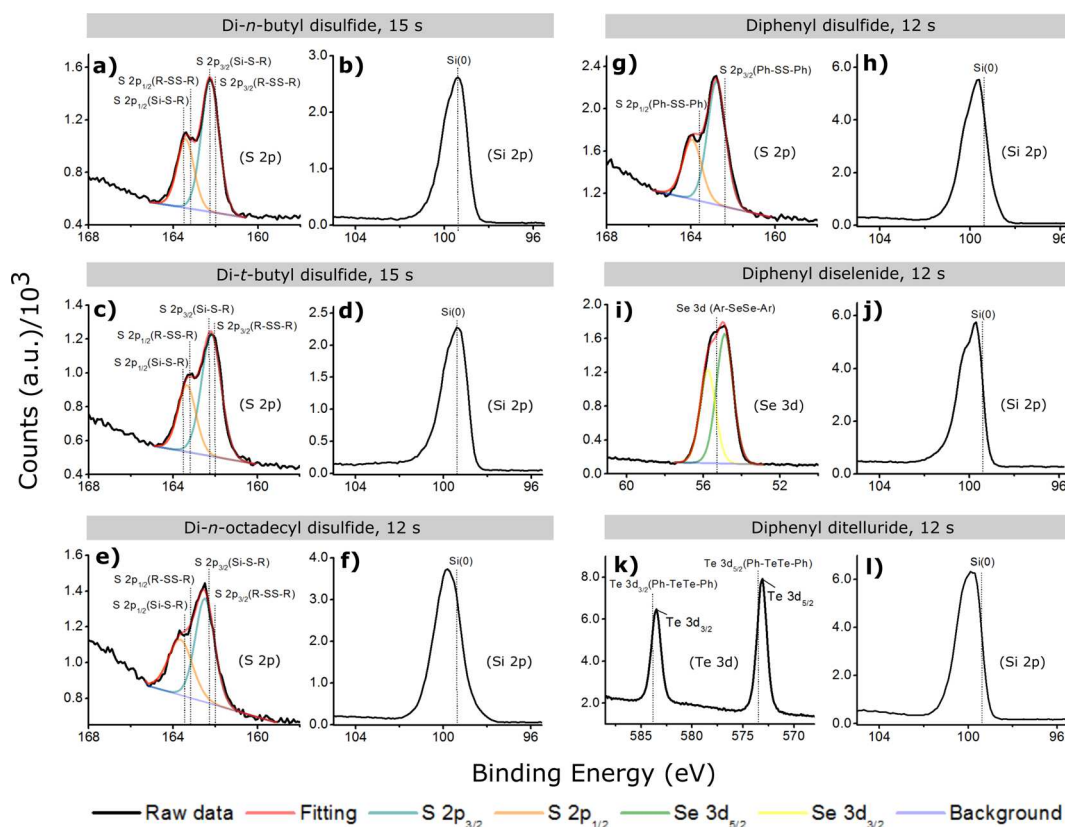


Figure 3. XPS of porous silicon samples after reaction with (a–h) the disulfide reagents, (i and j) diphényl diselenide, and (k and l) diphényl ditelluride for the times indicated with microwave irradiation. The data from this figure and supporting literature references are tabulated in Tables S1 and S2.

main text. The full series of spectra for each compound with different thermal treatment times is shown in Figures S1–S17. Functionalized surfaces were determined to have low oxidation levels by comparing the $\nu(\text{Si}-\text{O})$ feature at $1000\text{--}1100\text{ cm}^{-1}$ to that of the freshly etched, unfunctionalized porous silicon sample in Figure 2a, as well as the features corresponding to the $\nu(\text{Si}-\text{H}_x)$ of oxygen-back-bonded Si–H groups above 2200 cm^{-1} that result from oxygen insertion into nearby Si–Si bonds.^{41,52} In all cases, the broad compilation of $\nu(\text{Si}-\text{H}_x)$ modes, centered around 2100 cm^{-1} , decreases in intensity upon reaction. The three RSSR molecules, where R is aliphatic (Figure 2b–g, R = *n*-butyl, *t*-butyl, and *n*-octadecyl), exhibit profiles for their $\nu(\text{C}-\text{H}_x)$ modes in the region of $2850\text{--}2960\text{ cm}^{-1}$ that correspond to their respective functional groups upon comparison to the FTIR spectra of the neat parent chalcogenide molecules. The linear di-*n*-butyl and di-*n*-octadecyl disulfides react cleanly without obvious oxidation (Figure 2b,c,f,g). The highly hindered di-*t*-butyl disulfide, however, consistently shows some oxidation in the $\nu(\text{Si}-\text{O})$ stretching region at $\sim 1000\text{ cm}^{-1}$ upon microwave irradiation (Figure 2d), as well as the appearance of a small feature corresponding to oxygen-back-bonded Si–H_x groups above 2200 cm^{-1} and requires more time (15 s of microwave irradiation versus 10 or 12 s for all other reagents). Less oxidation is noted, however, for the hot plate reaction of di-*t*-butyl disulfide (Figure 2e). The diphényl chalcogenides, PhSSPh, PhSeSePh, and PhTeTePh, all reacted cleanly to yield FTIR spectra corresponding to expected modes of a phenyl ring, presumably Ph–S–Si≡, Ph–Se–Si≡, and Ph–Te–Si≡ moieties, with little oxidation.

To determine the elemental nature of the bond to the silicon (S, Se, or Te), and the level of oxidation, X-ray photoelectron spectroscopy (XPS) was carried out. The RSSR molecules all result in sulfur incorporation on the silicon surfaces (Figures 3a,c,e,g, and S20), the energy of which corresponds to the known binding energy of $\equiv\text{Si}-\text{S}-\text{R}$ groups.^{31,37} The corresponding silicon Si 2p spectra reveal little oxidation, which would appear as conspicuous higher energy features above 102 eV .^{5,53} The XPS spectra of the products of the reaction of PhSeSePh and PhTeTePh are shown in Figure 3i–l and reveal the presence of Se and Te, respectively, with little accompanying oxidation, at the expected binding energies.^{37,54} The disulfide molecule, bis(4-chlorophenyl) disulfide, which has a chlorine tag, was also reacted with the porous silicon, and the distinctive Cl 2p doublet was observed at 200.6 and 202.2 eV, in addition to the sulfur feature (Figure S20). XPS data for the chalcogenide features of the starting materials (molecules REER, E = S, Se, and Te), as well as reported values for $\equiv\text{Si}-\text{ER}$ when known, are shown in Figure 3 and Tables S1 and S2.

XPS analyses were complemented by depth profiling with ToF-SIMS, which provides information regarding elemental content, uniformity of functionalization throughout the layer, and comparative information regarding substitution levels. In all of the ToF-SIMS spectra shown here (Figure 4a–f), the baseline carbon level of a freshly etched porous silicon sample is shown (dotted black line) in each panel for comparison. It should be noted that because of the thickness of the porous silicon layer ($20\text{ }\mu\text{m}$) on the bulk wafer, the 2500 s of etching by ToF-SIMS here does not reach the porous silicon–bulk silicon interface. As can be seen for the porous silicon samples

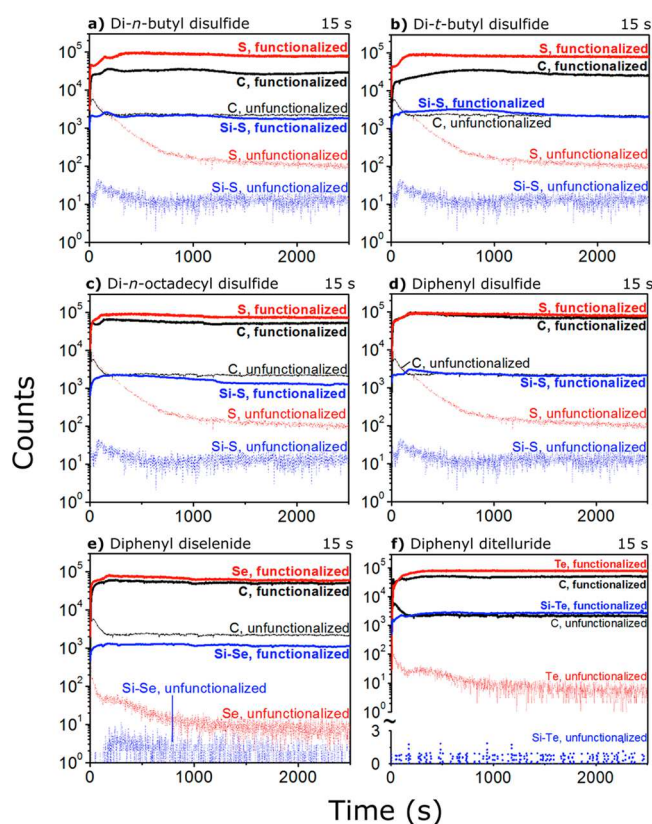


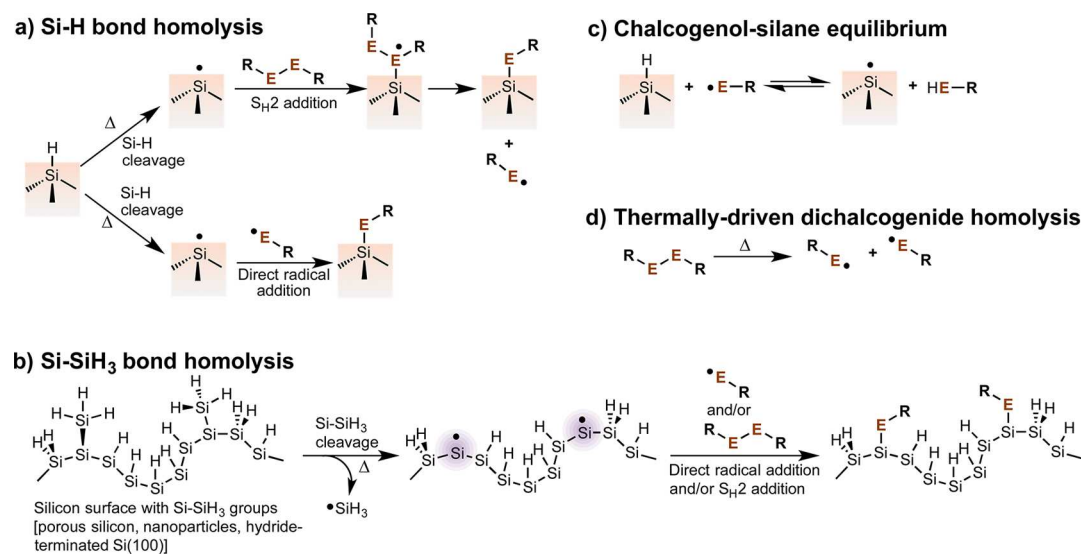
Figure 4. ToF-SIMS analysis of functionalized porous silicon samples. The thick curves represent the porous silicon samples after reaction with (a–d) the disulfide reagents, (e) diphenyl diselenide, and (f) diphenyl ditelluride, all under microwave irradiation for 15 s. The same sample of unfunctionalized porous silicon was used as the comparison (reference sample, dotted line) in all spectra.

functionalized disulfides, RSSR (Figure 4a–d), the level of carbon and sulfur increases by one or more orders of

magnitude when contrasted with the unfunctionalized control. The substitution levels appear consistent and flat throughout the porous silicon film. The diphenyl diselenide- and ditelluride-functionalized porous silicon surfaces show similar results for both carbon and Se and Te, respectively (Figure 4e,f). Bis(4-chlorophenyl) disulfide, with its chlorine label, was also reacted with porous silicon and shows 2–3 orders of magnitude increase in the level of chlorine compared to that of the unfunctionalized control, as well as much higher levels of carbon and sulfur (Figure S21). In all cases, the levels corresponding to the Si–E fragments (E = S, Se, and Te) increase by 2 orders of magnitude over those in the unfunctionalized sample, providing further evidence to support the claim of a $\equiv\text{Si}-\text{E}$ bond.

Mechanism. Possible reactions that could play a role in the mechanism of $\equiv\text{Si}-\text{E}$ (E = S, Se, and Te) bond formation on silicon surfaces are shown in Scheme 2. Four different reactions need to be considered, including thermally driven homolytic silicon–hydrogen bond and silicon–silicon bond cleavage (Schemes 2a,b), well-established radical equilibria between thiols and silanes (Scheme 2c), and dichalcogenide homolysis to cleave the E–E bond (Scheme 2d). Because there is a rich body of literature pertaining to the molecular reactivity of disulfides with silane radicals,^{55–59} it is proposed that the key intermediate is the surface silyl radical, or dangling bond, represented by $\equiv\text{Si}\cdot$. This surface radical can be accessed via three possible routes. The first route is a direct thermally driven homolytic bond cleavage, as shown in Scheme 2a, which has been postulated as a key step in thermally driven hydrosilylation on hydride surfaces.^{60,61} The second route to a surface-bound $\equiv\text{Si}\cdot$ is the more recently proposed Si–Si bond cleavage of $\equiv\text{Si}-\text{SiH}_3$ species, resulting in loss of $\cdot\text{SiH}_3$, shown in Scheme 2b.⁶² Porous silicon is terminated with $\equiv\text{SiH}$, $=\text{SiH}_2$, and $-\text{SiH}_3$ groups, of which the single Si–Si bond is the weakest bond present (bond dissociation energy is 70–80 kcal/mol)⁶³ compared to the Si–H bonds (bond dissociation

Scheme 2. Possible Mechanisms That Could Play a Role in Formation of $\equiv\text{Si}-\text{E}$ Bonds (E = S, Se, and Te) on Silicon Surfaces^a



^a(a) Direct homolysis of Si–H bonds by heat, leading to formation of silicon radicals on the surface, and subsequent reaction with a dichalcogenide or a chalcogenyl radical. (b) Scheme for homolysis of Si–SiH₃ bonds on the surface, leading to silicon radicals. (c) Radical-based chalcogenol-silane equilibrium. (d) Homolysis of dichalcogenides, leading to chalcogenyl radical formation.

energies of 85–90 kcal/mol).⁶³ Neale and co-workers⁶² have shown that cleavage of $\equiv\text{Si}-\text{SiH}_3$ groups on hydride-terminated silicon nanoparticles may be the dominant initiation step for hydrosilylation with alkenes. The third route to formation of $\equiv\text{Si}\cdot$ is removal of the silicon-bound H \cdot by a chalcogenyl radical, shown in Scheme 2c.^{58,62,64} The thiyl, selenyl, and telluryl radicals would result from homolysis of the weak S–S, Se–Se, or Te–Te bond, which have bond dissociation energies of 53–57, ~40, and ~30–35 kcal/mol, respectively, under these high-temperature conditions (Scheme 2d).⁶⁵ Thiyl and selenyl radicals are known radical propagators, and presumably telluryl radicals would play a similar role, plucking hydrogen atoms from the silicon surface to produce silyl surface radicals, particularly under high concentrations of reagents.^{66–68}

Assuming the central role of the $\equiv\text{Si}\cdot$ radical species, the formation of the $\equiv\text{Si}-\text{E}$ bond could occur through two possible pathways. As is well-established in the molecular silane radical literature,^{37,56} dialkyl and diaryl disulfides and diselenides can add to the silyl radical through an $\text{S}_{\text{H}2}$ mechanism (Scheme 2a), producing a sulfuranyl or seleranyl intermediate that then collapses to form the $\equiv\text{Si}-\text{ER}$ final product, releasing an equivalent of $\cdot\text{ER}$ (E = S and Se). The equilibria between silanes and thiols under radical conditions have been extensively studied, and although there are few examples of direct coupling of a silane radical, $\equiv\text{Si}\cdot$, and a chalcogenide radical, $\cdot\text{ER}$, to produce $\equiv\text{Si}-\text{ER}$ bonds, there is precedent.⁶⁹ Thus, the possibility of direct coupling is shown in Scheme 2a.

To help provide insight into the mechanism, the reactivity of the alkanethiols, 1-octadecanethiol and *t*-butyl thiol, via microwave heating was examined by FTIR and XPS (shown in Figures S7, S8, S16, S17, S19, and S20). Both reactions resulted in low incorporation levels on the basis of comparison with the spectra of the reaction with di-*n*-octadecyl disulfide (Figure 2f,g), in spite of a slightly longer exposure to microwave irradiation (10 s for the disulfide versus 15 s for the thiol). The low yield of $\equiv\text{Si}-\text{SR}$ formation with the thiol precursor compared to that of the corresponding dialkyl disulfide suggests that the stronger S–H bond⁷⁰ (bond dissociation energy \approx 84 kcal/mol) translates to lower yields of the homolysis product, $\text{RS}\cdot$, and hence slower kinetics. Korgel and co-workers recently proposed that during the thermal reaction of dodecanethiol with hydrogen-terminated silicon nanoparticles, the thiol could be oxidized in situ to produce di-*n*-dodecyl disulfide, which then reacts with the surface.³⁶ Although the mechanism involving dichalcogenides proposed here requires further investigation, it appears that the dialkyl and diaryl disulfides are more reactive under these conditions than the corresponding thiols and that this difference of reactivity could be due to the ease of homolysis of the dichalcogenide bond, E–E, compared to that of the RE–H bond, which then enables radicals to propagate and react.

CONCLUSIONS

In this work, we described a very fast thermal functionalization strategy for silicon surfaces to enable the covalent interfacing of molecules and self-assembled monolayers through $\equiv\text{Si}-\text{ER}$ bonds, where E = S, Se, and Te. Through either a microwave or hot plate thermal heating approach with dichalcogenide compounds that contain S–S, Se–Se, or Te–Te bonds, well-defined molecular bonds with low levels of oxidation are easily produced. The alkyl and aryl dichalcogenide molecules are

practical to work with because they are stable, commercially available, and of low odor compared to thiols. The series of chalcogen–silicon bonds, from Si–O, to Si–S, to Si–Se, and now to Si–Te, can now be easily accessed and applied to a variety of electronic applications on this semiconductor. Modulation of work function, monolayer doping of silicon, and expansion of the repertoire of hybrid organic–semiconductor electronic devices is possible through this applied surface chemical approach.

ASSOCIATED CONTENT

Supporting Information

The Supporting Information is available free of charge on the ACS Publications website at DOI: 10.1021/acsami.6b00784.

FTIR spectra of porous silicon reactions with varying time, complementary XPS data, SEM micrographs of the porous silicon samples, and photographs of experimental apparatus. (PDF)

AUTHOR INFORMATION

Corresponding Author

*E-mail: jburia@ualberta.ca.

Funding

This work was supported by grants from the Natural Sciences and Engineering Research Council (NSERC, grant numbers RGPIN-283291-09 and RGPIN-2014-05195), Alberta Innovates Technology Futures (fellowships to M.H. and F.L., and grant number AITF iCORE IC50-T1 G2013000198), the China Scholarship Council (fellowship to F.L.), and the Canada Research Chairs program (CRC 207142, to J.M.B.). Electron microscopy was carried out NRC-NINT.

Notes

The authors declare no competing financial interest.

ACKNOWLEDGMENTS

We thank Tate Hauger for experimental assistance.

REFERENCES

- (1) Jeong, M.; Doris, B.; Kedzierski, J.; Rim, K.; Yang, M. Silicon Device Scaling to the Sub-10-nm Regime. *Science* **2004**, *306*, 2057–2060.
- (2) Tao, F.; Zhu, Y.; Bernasek, S. L. In *Functionalization of Semiconductor Surfaces*; Tao, F., Bernasek, S. L., Eds.; Wiley: Hoboken, NJ, 2012; Chapter 1, pp 1–10.
- (3) Dasog, M.; Kehrle, J.; Rieger, B.; Veinot, J. G. C. Silicon Nanocrystals and Silicon-Polymer Hybrids: Synthesis, Surface Engineering, and Applications. *Angew. Chem., Int. Ed.* **2016**, *55*, 2322–2339.
- (4) Peng, F.; Su, Y.; Zhong, Y.; Fan, C.; Lee, S.-T.; He, Y. Silicon Nanomaterials Platform for Bioimaging, Biosensing, and Cancer Therapy. *Acc. Chem. Res.* **2014**, *47*, 612–623.
- (5) Bruce, J. P.; Oliver, D. R.; Lewis, N. S.; Freund, M. S. Electrical Characteristics of the Junction between PEDOT:PSS and Thiophene-Functionalized Silicon Microwires. *ACS Appl. Mater. Interfaces* **2015**, *7*, 27160–27166.
- (6) Cheng, X.; Lowe, S. B.; Reece, P. J.; Gooding, J. J. Colloidal Silicon Quantum Dots: From Preparation to the Modification of Self-Assembled Monolayers (SAMs) for Bio-Applications. *Chem. Soc. Rev.* **2014**, *43*, 2680–2700.
- (7) Paul, A.; Jana, A.; Karthik, S.; Bera, M.; Zhao, Y.; Singh, N. D. P. Photoresponsive Real Time Monitoring Silicon Quantum Dots for Regulated Delivery of Anticancer Drugs. *J. Mater. Chem. B* **2016**, *4*, 521–528.

- (8) Kang, O. S.; Bruce, J. P.; Herbert, D. E.; Freund, M. S. Covalent Attachment of Ferrocene to Silicon Microwire Arrays. *ACS Appl. Mater. Interfaces* **2015**, *7*, 26959–26967.
- (9) Ciampi, S.; Choudhury, M. H.; Ahmad, S. A. B. A.; Darwish, N.; Brun, A. L.; Gooding, J. J. The Impact of Surface Coverage on the Kinetics of Electron Transfer through Redox Monolayers on a Silicon Electrode Surface. *Electrochim. Acta* **2015**, *186*, 216–222.
- (10) Vilan, A.; Yaffe, O.; Biller, A.; Salomon, A.; Kahn, A.; Cahen, D. Molecules on Si: Electronics with Chemistry. *Adv. Mater.* **2010**, *22*, 140–159.
- (11) Wang, J.; Zhou, Y.; Watkinson, M.; Gautrot, J.; Krause, S. High-Sensitivity Light-Addressable Potentiometric Sensors Using Silicon on Sapphire Functionalized with Self-Assembled Organic Monolayers. *Sens. Actuators, B* **2015**, *209*, 230–236.
- (12) Kanyong, P.; Sun, G.; Rösicke, F.; Syritski, V.; Panne, U.; Hinrichs, K.; Rappich, J. Maleimide Functionalized Silicon Surfaces for Biosensing Investigated by in-Situ IRSE and EQCM. *Electrochem. Commun.* **2015**, *51*, 103–107.
- (13) Dasog, M.; Bader, K.; Veinot, J. G. C. Influence of Halides on the Optical Properties of Silicon Quantum Dots. *Chem. Mater.* **2015**, *27*, 1153–1156.
- (14) Fermi, A.; Locritani, M.; Di Carlo, G.; Pizzotti, M.; Caramori, S.; Yu, Y.; Korgel, B. A.; Bergamini, G.; Ceroni, P. Light-Harvesting Antennae Based on Photoactive Silicon Nanocrystals Functionalized with Porphyrin Chromophores. *Faraday Discuss.* **2015**, *185*, 481–495.
- (15) Peng, W.; Rupich, S. M.; Shafiq, N.; Gartstein, Y. N.; Malko, A. V.; Chabal, Y. J. Silicon Surface Modification and Characterization for Emergent Photovoltaic Applications Based on Energy Transfer. *Chem. Rev.* **2015**, *115*, 12764–12796.
- (16) Wong, K. T.; Lewis, N. S. What a Difference a Bond Makes: The Structural, Chemical, and Physical Properties of Methyl-Terminated Si(111) Surfaces. *Acc. Chem. Res.* **2014**, *47*, 3037–3044.
- (17) Brown, E. S.; Hlynchuk, S.; Maldonado, S. Chemically Modified Si(111) Surfaces Simultaneously Demonstrating Hydrophilicity, Resistance against Oxidation, and Low Trap State Densities. *Surf. Sci.* **2016**, *645*, 49–55.
- (18) Toledano, T.; Garrick, R.; Sinai, O.; Bendikov, T.; Haj-Yahia, A.-E.; Lerman, K.; Alon, H.; Sukenik, C. N.; Vilan, A.; Kronik, L.; Cahen, D. Effect of Binding Group on Hybridization across the Silicon/aromatic-Monolayer Interface. *J. Electron Spectrosc. Relat. Phenom.* **2015**, *204*, 149–158.
- (19) Li, F.; Basile, V. M.; Rose, M. J. Electron Transfer through Surface-Grown, Ferrocene-Capped Oligophenylene Molecular Wires (5–50 Å) on N-Si(111) Photoelectrodes. *Langmuir* **2015**, *31*, 7712–7716.
- (20) DeBenedetti, W. J. I.; Chiu, S.-K.; Radlinger, C. M.; Ellison, R. J.; Manhat, B. A.; Zhang, J. Z.; Shi, J.; Goforth, A. M. Conversion from Red to Blue Photoluminescence in Alcohol Dispersions of Alkyl-Capped Silicon Nanoparticles: Insight into the Origins of Visible Photoluminescence in Colloidal Nanocrystalline Silicon. *J. Phys. Chem. C* **2015**, *119*, 9595–9608.
- (21) Arefi, H. H.; Fagas, G. Chemical Trends in the Work Function of Modified Si(111) Surfaces: A DFT Study. *J. Phys. Chem. C* **2014**, *118*, 14346–14354.
- (22) Cooper, A. J.; Keyvanfar, K.; Deberardinis, A.; Pu, L.; Bean, J. C. Dopant Passivation and Work Function Tuning through Attachment of Heterogeneous Organic Monolayers on Silicon in Ultrahigh Vacuum. *Appl. Surf. Sci.* **2011**, *257*, 6138–6144.
- (23) Arefi, H. H.; Nolan, M.; Fagas, G. Role of the Head And/or Tail Groups of Adsorbed $-[X^{\text{head group}}]\text{-Alkyl-}[X^{\text{tail group}}]$ [$X = \text{O}(\text{H}), \text{S}(\text{H}), \text{NH}_{(2)}$] Chains in Controlling the Work Function of the Functionalized H:Si(111) Surface. *J. Phys. Chem. C* **2015**, *119*, 11588–11597.
- (24) Yasserli, A. A.; Syomin, D.; Loewe, R. S.; Lindsey, J. S.; Zaera, F.; Bocian, D. F. Structural and Electron-Transfer Characteristics of O-, S-, and Se-Tethered Porphyrin Monolayers on Si(100). *J. Am. Chem. Soc.* **2004**, *126*, 15603–15612.
- (25) Sieval, A. B.; Demirel, A. L.; Nissink, J. W. M.; Linford, M. R.; van der Maas, J. H.; de Jeu, W. H.; Zuilhof, H.; Sudhölter, E. J. R. Highly Stable Si–C Linked Functionalized Monolayers on the Silicon (100) Surface. *Langmuir* **1998**, *14*, 1759–1768.
- (26) Yang, Z.; Gonzalez, C. M.; Purkait, T. K.; Iqbal, M.; Meldrum, A.; Veinot, J. G. C. Radical Initiated Hydrosilylation on Silicon Nanocrystal Surfaces: An Evaluation of Functional Group Tolerance and Mechanistic Study. *Langmuir* **2015**, *31*, 10540–10548.
- (27) Steinrück, H.-G.; Schiener, A.; Schindler, T.; Will, J.; Magerl, A.; Kononov, O.; Li Destri, G.; Seeck, O. H.; Mezger, M.; Haddad, J.; Deutsch, M.; Checco, A.; Ocko, B. M. Nanoscale Structure of Si/SiO₂/Organics Interfaces. *ACS Nano* **2014**, *8*, 12676–12681.
- (28) Gusev, E. P.; Lu, H. C.; Gustafsson, T.; Garfunkel, E. Growth Mechanism of Thin Silicon Oxide Films on Si(100) Studied by Medium-Energy Ion Scattering. *Phys. Rev. B: Condens. Matter Mater. Phys.* **1995**, *52*, 1759–1775.
- (29) Yu, L. H.; Gergel-Hackett, N.; Zangmeister, C. D.; Hacker, C. A.; Richter, C. A.; Kushmerick, J. G. Molecule-Induced Interface States Dominate Charge Transport in Si-alkyl-metal Junctions. *J. Phys.: Condens. Matter* **2008**, *20*, 374114.
- (30) Huang, Y.-S.; Chen, C.-H.; Chen, C.-H.; Hung, W.-H. Fabrication of Octadecyl and Octadecanethiolate Self-Assembled Monolayers on Oxide-Free Si(111) with a One-Cell Process. *ACS Appl. Mater. Interfaces* **2013**, *5*, 5771–5776.
- (31) Lou, J. L.; Shiu, H. W.; Chang, L. Y.; Wu, C. P.; Soo, Y.-L.; Chen, C.-H. Preparation and Characterization of an Ordered 1-Dodecanethiol Monolayer on Bare Si(111) Surface. *Langmuir* **2011**, *27*, 3436–3441.
- (32) Hacker, C. A. Modifying Electronic Properties at the Silicon–molecule Interface Using Atomic Tethers. *Solid-State Electron.* **2010**, *54*, 1657–1664.
- (33) Sano, H.; Ohno, K.; Ichii, T.; Murase, K.; Sugimura, H. Alkanethiol Self-Assembled Monolayers Formed on Silicon Substrates. *Jpn. J. Appl. Phys.* **2010**, *49*, 01AE09.
- (34) Balakumar, A.; Lysenko, A. B.; Carcel, C.; Malinovsky, V. L.; Gryko, D. T.; Schweikart, K.-H.; Loewe, R. S.; Yasserli, A. A.; Liu, Z.; Bocian, D. F.; Lindsey, J. S. Diverse Redox-Active Molecules Bearing O-, S-, or Se-Terminated Tethers for Attachment to Silicon in Studies of Molecular Information Storage. *J. Org. Chem.* **2004**, *69*, 1435–1443.
- (35) Yasserli, A. A.; Syomin, D.; Loewe, R. S.; Lindsey, J. S.; Zaera, F.; Bocian, D. F. Structural and Electron-Transfer Characteristics of O-, S-, and Se-Tethered Porphyrin Monolayers on Si(100). *J. Am. Chem. Soc.* **2004**, *126*, 15603–15612.
- (36) Yu, Y.; Rowland, C. E.; Schaller, R. D.; Korgel, B. A. Synthesis and Ligand Exchange of Thiol-Capped Silicon Nanocrystals. *Langmuir* **2015**, *31*, 6886–6893.
- (37) Buriak, J. M.; Sikder, M. D. H. From Molecules to Surfaces: Radical-Based Mechanisms of Si–S and Si–Se Bond Formation on Silicon. *J. Am. Chem. Soc.* **2015**, *137*, 9730–9738.
- (38) Dabbousi, B. O.; Bonasia, P. J.; Arnold, J. Tris(trimethylsilyl)silanetellurol: Preparation, Characterization, and Synthetic Utility of a Remarkably Stable Tellurol. *J. Am. Chem. Soc.* **1991**, *113*, 3186–3188.
- (39) Sadekov, I. D.; Zakharov, A. V. Stable Tellurols and Their Metal Derivatives. *Russ. Chem. Rev.* **1999**, *68*, 909–923.
- (40) Ferreira, J. T. B.; De Oliveira, A. R. M.; Comassetto, J. V. A Convenient Method of Synthesis of Dialkyltellurides and Dialkylid-tellurides. *Synth. Commun.* **1989**, *19*, 239–244.
- (41) Buriak, J. M.; Stewart, M. P.; Geders, T. W.; Allen, M. J.; Choi, H. C.; Smith, J.; Raftery, D.; Canham, L. T. Lewis Acid Mediated Hydrosilylation on Porous Silicon Surfaces. *J. Am. Chem. Soc.* **1999**, *121*, 11491–11502.
- (42) Sailor, M. J. *Porous Silicon in Practice*; Wiley-VCH: Weinheim, 2011; Chapter 2, pp 43–76.
- (43) Jin, C.; Murphy, J. N.; Harris, K. D.; Buriak, J. M. Deconvoluting the Mechanism of Microwave Annealing of Block Copolymer Thin Films. *ACS Nano* **2014**, *8*, 3979–3991.
- (44) Sailor, M. J. In *Handbook of Porous Silicon*; Canham, L., Ed.; Springer: Basel, Switzerland, 2014; Part II, pp 355–380.
- (45) Huck, L. A.; Buriak, J. M. In *Handbook of Porous Silicon*; Canham, L., Ed.; Springer: Basel, Switzerland, 2014; Part IV, pp 683–693.

- (46) Ogata, Y. H. In *Handbook of Porous Silicon*; Canham, L., Ed.; Springer: Basel, Switzerland, 2014; Part III, pp 473–480.
- (47) Chabal, Y. J.; Higashi, G. S.; Raghavachari, K.; Burrows, V. A. Infrared Spectroscopy of Si(111) and Si(100) Surfaces after HF Treatment: Hydrogen Termination and Surface Morphology. *J. Vac. Sci. Technol., A* **1989**, *7*, 2104–2109.
- (48) Yu, Y.; Hessel, C. M.; Bogart, T. D.; Panthani, M. G.; Rasch, M. R.; Korgel, B. A. Room Temperature Hydrosilylation of Silicon Nanocrystals with Bifunctional Terminal Alkenes. *Langmuir* **2013**, *29*, 1533–1540.
- (49) Buriak, J. M. Organometallic Chemistry on Silicon and Germanium Surfaces. *Chem. Rev.* **2002**, *102*, 1271–1308.
- (50) Yu, Y.; Korgel, B. A. Controlled Styrene Monolayer Capping of Silicon Nanocrystals by Room Temperature Hydrosilylation. *Langmuir* **2015**, *31*, 6532–6537.
- (51) Boukherroub, R.; Petit, A.; Loupy, A.; Chazalviel, J.-N.; Ozanam, F. Microwave-Assisted Chemical Functionalization of Hydrogen-Terminated Porous Silicon Surfaces. *J. Phys. Chem. B* **2003**, *107*, 13459–13462.
- (52) Riikonen, J.; Salomäki, M.; van Wonderen, J.; Kemell, M.; Xu, W.; Korhonen, O.; Ritala, M.; MacMillan, F.; Salonen, J.; Lehto, V.-P. Surface Chemistry, Reactivity, and Pore Structure of Porous Silicon Oxidized by Various Methods. *Langmuir* **2012**, *28*, 10573–10583.
- (53) Nemanick, E. J.; Hurley, P. T.; Webb, L. J.; Knapp, D. W.; Michalak, D. J.; Brunshwig, B. S.; Lewis, N. S. Chemical and Electrical Passivation of Single-Crystal Silicon(100) Surfaces through a Two-Step Chlorination/Alkylation Process. *J. Phys. Chem. B* **2006**, *110*, 14770–14778.
- (54) Santucci, S.; Di Nardo, S.; Lozzi, L.; Passacantando, M.; Picozzi, P. XPS, LEED and AFM Investigation of the Si(100) Surface after the Deposition and Annealing of Tellurium Thin Films. *Surf. Sci.* **1996**, *352–354*, 1027–1032.
- (55) Ballestri, M.; Chatgililoglu, C.; Clark, K. B.; Griller, D.; Giese, B.; Kopping, B. Tris(trimethylsilyl)silane as a Radical-Based Reducing Agent in Synthesis. *J. Org. Chem.* **1991**, *56*, 678–683.
- (56) Chatgililoglu, C. Structural and Chemical Properties of Silyl Radicals. *Chem. Rev.* **1995**, *95*, 1229–1251.
- (57) Chatgililoglu, C. The Tris(trimethylsilyl)silane/Thiol Reducing System: A Tool for Measuring Rate Constants for Reactions of Carbon-Centered Radicals with Thiols. *Helv. Chim. Acta* **2006**, *89*, 2387–2398.
- (58) Chatgililoglu, C. $(\text{Me}_3\text{Si})_3\text{SiH}$: Twenty Years After Its Discovery as a Radical-Based Reducing Agent. *Chem. - Eur. J.* **2008**, *14*, 2310–2320.
- (59) Zavitsas, A. A.; Chatgililoglu, C. Energies of Activation. The Paradigm of Hydrogen Abstractions by Radicals. *J. Am. Chem. Soc.* **1995**, *117*, 10645–10654.
- (60) Linford, M. R.; Fenter, P.; Eisenberger, P. M.; Chidsey, C. E. D. Alkyl Monolayers on Silicon Prepared from 1-Alkenes and Hydrogen-Terminated Silicon. *J. Am. Chem. Soc.* **1995**, *117*, 3145–3155.
- (61) de Smet, L. C. P. M.; Zuilhof, H.; Sudhölter, E. J. R.; Lie, L. H.; Houlton, A.; Horrocks, B. R. Mechanism of the Hydrosilylation Reaction of Alkenes at Porous Silicon: Experimental and Computational Deuterium Labeling Studies. *J. Phys. Chem. B* **2005**, *109*, 12020–12031.
- (62) Wheeler, L. M.; Anderson, N. C.; Palomaki, P. K. B.; Blackburn, J. L.; Johnson, J. C.; Neale, N. R. Silyl Radical Abstraction in the Functionalization of Plasma-Synthesized Silicon Nanocrystals. *Chem. Mater.* **2015**, *27*, 6869–6878.
- (63) Walsh, R. Bond Dissociation Energy Values in Silicon-Containing Compounds and Some of Their Implications. *Acc. Chem. Res.* **1981**, *14*, 246–252.
- (64) Dénès, F.; Pichowicz, M.; Povie, G.; Renaud, P. Thiyl Radicals in Organic Synthesis. *Chem. Rev.* **2014**, *114*, 2587–2693.
- (65) McDonough, J. E.; Weir, J. J.; Sukcharoenphon, K.; Hoff, C. D.; Kryatova, O. P.; Rybak-Akimova, E. V.; Scott, B. L.; Kubas, G. J.; Mendiratta, A.; Cummins, C. C. Comparison of Thermodynamic and Kinetic Aspects of Oxidative Addition of PhE-EPh ($\text{E} = \text{S}, \text{Se}, \text{Te}$) to $\text{Mo}(\text{CO})_3(\text{PR}_3)_2$, $\text{W}(\text{CO})_3(\text{PR}_3)_2$, and $\text{Mo}(\text{N}[\text{tBu}]\text{Ar})_3$ Complexes. The Role of Oxidation State and Ancillary Ligands in Metal Complex Induced Chalcogenyl Radical Generation. *J. Am. Chem. Soc.* **2006**, *128*, 10295–10303.
- (66) Subramanian, H.; Moorthy, R.; Sibi, M. P. Thiyl Radicals: From Simple Radical Additions to Asymmetric Catalysis. *Angew. Chem., Int. Ed.* **2014**, *53*, 13660–13662.
- (67) Ogawa, A. In *Main Group Metals in Organic Synthesis*; Yamamoto, H., Oshima, K., Eds.; Wiley-VCH: Weinheim, 2004; Chapter 15, pp 813–866.
- (68) Renaud, P. In *Topics in Current Chemistry: Organoselenium Chemistry*; Wirth, D. T., Ed.; Springer: Berlin, 2000; Chapter 4, pp 81–112.
- (69) Wittenberg, D.; McNinch, H. A.; Gilman, H. The Reaction of Some Silicon Hydrides with Sulfur-Containing Heterocycles and Related Compounds. *J. Am. Chem. Soc.* **1958**, *80*, 5418–5422.
- (70) Oae, S.; Doi, J. In *Organic Sulfur Chemistry: Structure and Mechanisms*; CRC Press: Boca Raton, FL, 1991.